THE JOURNAL OF PHYSICAL CHEMISTRY B

Article

pubs.acs.org/JPCB

Comparative Experimental and Computational Study of Monoalkyl Chain Phosphatidylcholine-Containing Thermoresponsive Liposomes

Kleopatra Eleftheriou,[†] Zili Sideratou,[†] Angelos Thanassoulas,[‡] Athanasios Papakyriakou,[†] and Dimitris Tsiourvas*[,†]

[†]Institute of Nanoscience and Nanotechology, NCSR "Demokritos", 15310 Aghia Paraskevi, Attiki, Greece

[‡]Institute of Nuclear & Radiological Sciences and Technology, Energy & Safety, NCSR "Demokritos", 15310 Aghia Paraskevi, Attiki, Greece

Supporting Information

ABSTRACT: Liposomes containing lysophospholipids are intensively studied as drug delivery systems that are stable at normal body temperature but exhibit fast release of their drug load at slightly elevated temperatures. In this study, the stability and release properties of dipalmitoylglycerophosphocholine (DPPC)-based liposomes incorporating the commonly used lysophosphatidylocholine (lyso-PC), and a series of monoalkyl chain ether-linked phosphatidylcholine, i.e., the biologically relevant monoalkyl chain platelet activating factor (PAF) and its derivatives lyso-PAF and methyl-PAF, were investigated. To this end a series of PEGylated small unilamellar liposomes with DPPC:monoalkyl lipid compositions of 5% and 10% molar ratio were prepared and compared with regard to stability (37 °C) and release properties at elevated temperatures (38−43 °C). All systems were characterized with respect to size distribution, ζ-potential, and phase transition characteristics. The presence of ether−lipids endows liposomes with superior (∼10% increase) release properties at 5% incorporation compared to lyso-PC, while at 10% molar ratio the formulations do not differ significantly, the release being close to 90%. The findings are supported by atomistic molecular dynamics simulations that suggest a correlation between the enhanced permeability and increased penetration of water molecules within the bilayers with density fluctuations resulting from the increased area-per-lipid and the disorder of the lysolipids alkyl chains.

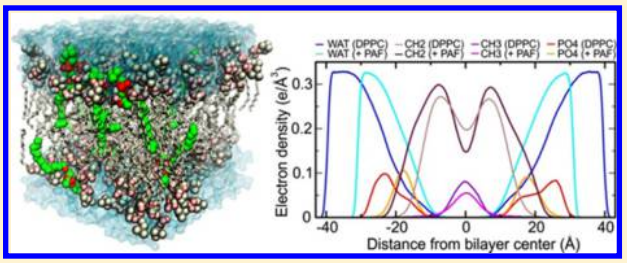

1. INTRODUCTION

Local hyperthermia therapy, a therapy in which a tissue is heated at temperatures higher than the normal, is considered as a promising tool in cancer treatment, complementing and increasing the efficacy of anticancer drugs. Topically increased temperature treatments, such as microwave irradiation, high-intensity focused ultrasounds, or radiofrequency thermal ablation, result in improved tumor blood flow, vascular permeability, and upregulated drug influx in the tumor.[1,2] A therapeutic advantage is foreseen when mild hyperthermia (40−41 °C) is combined with suitably designed thermally triggered drug delivery systems, as in this case the drug load would be released almost exclusively in the heated tumor, achieving locally high active ingredient concentrations and avoiding its release in nonmalignant tissues which further minimizes drug side effects. To this end a number of thermoresponsive drug delivery systems have been tested,[3] among which a large number of liposomal formulations.

In a seminal work, Papahadjopoulos et al.[4] showed that the liposomal bilayer membrane becomes permeable at temperatures in the vicinity of the main gel to liquid crystal phase transition temperature, T_m, but not below or above this temperature range. This property was soon exploited by the same laboratory,[5] as well as by other groups,[6,7] for achieving local and controlled release of liposomal encapsulated water-soluble drugs employing hyperthermia. The successful translation into clinical practice requires the development of liposomal formulations that are stable at temperatures less than 39 °C, release of their contents at clinically relevant temperatures (39.5−41.5 °C), and and achieve almost complete drug release within a short time frame. A major contribution to this objective was the work of Needham et al., who introduced the use of a lysophospholipid, i.e., a monoalkyl chain phosphatidylcholine (lyso-PC), to impart thermosensitive properties in dipalmitoylglycerophosphocholine (DPPC)-based liposomes.[8−11] Ever since, a significant number of various liposomal formulations have been studied, as summarized in several reviews,[12−14] which show that, in combination with hyperthermia, liposomal effectiveness and accumulation in tumors is maximized.[15,16] In most of these formulations, in order to avoid attack from the immune system and prolong the circulation time, the liposomal surface was modified with

Received: March 17, 2016
Revised: May 13, 2016

DOI: 10.1021/acs.jpcb.6b02783
J. Phys. Chem. B XXXX, XXX, XXX−XXX

poly(ethylene glycol) affording PEGylated liposomes, which have extended half-lives in the circulatory system.[17−19]

It is now widely accepted that the incorporation of specific molecules in the bilayer results in the formation of open membrane structures (pores) that appear to be thermodynamically stable near T_m.[15,16,18] Although new molecules of different structures, from simple surfactants, such as Brij,[20] lyso-lipids of various chemical structures,[21] or lipids having a phosphoglycerol headgroup,[17] to thermosensitive polymers, such as poly(*N*-isopropylacrylamide),[22] have been successfully tested for imparting thermoresponsive properties in the bilayers, liposomes containing lyso-PC are still considered the most advanced. In fact, this liposomal formulation encapsulating doxorubicin is currently being studied in phase 3 clinical trials under the trade name ThermoDox.[23]

In this study the effect of a series of monoalkyl chain ether-linked phosphatidylcholines, which are similar to lyso-PC, and specifically the platelet activating factor, PAF, and its derivatives lyso-PAF and methyl-PAF (Scheme I) on the thermoresponsive

Scheme I. Chemical Structures of DPPC and of Monoalkyl Chain Phosphatidylcholines

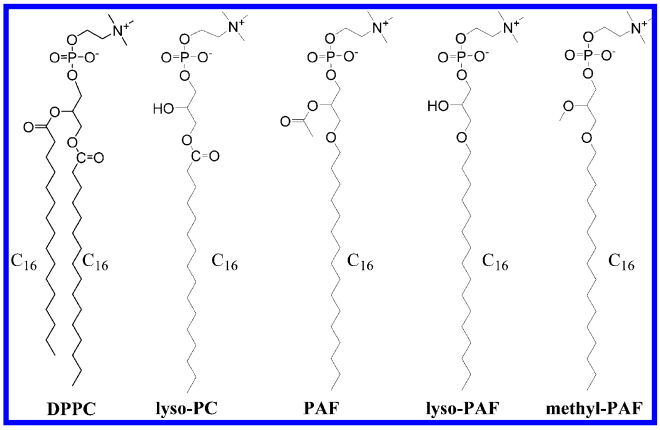

properties of DPPC liposomes was investigated. All of the members of this series differ from lyso-PC in the way that the alkyl chain is attached at the 1-position of the glycerol unit (ether bond vs ester bond). Within the series, the members differ in the substitution at the 2-position of glycerol group. PAF and lyso-PAF are naturally occurring lipids which have been previously suggested to be more potent than lyso-PC in the fluidization of the DPPC hydrated bilayers of multilamellar vesicles due both to the ether bond linkage at the 1-position of the glycerol unit and also to the groups present at the 2-position.[24,25] On the other hand, methyl-PAF is a synthetic PAF derivative with high metabolic stability and anticancer properties.[25] While it has been reported that the substitution of the ester bond of lyso-PC with an ether bond has very little effect on the overall thermotropic behavior, previous studies revealed that due to the significant double-bond character of the ester group in lyso-PC compared to the ether bond in PAF and its derivatives, the rotation about the O−C bond that links the long aliphatic chain with the polar region is considerably hindered compared to the ether bond. The presence of the ether bond allows more rotational freedom and, thus, reduces significantly the rigidity of the membrane.[24,26] Unilamellar liposomes consisting of DPPC and DSPE-PEG at 91:4 molar ratio were prepared also incorporating 5 and 10 mol % of ether-linked phosphatidylcholines with a hexadecyl alkyl chain, i.e., PAF, lyso-PAF, and methyl-PAF as well as the well-studied ester-linked lyso-PC, Scheme I, in an effort to establish a possible relationship between the chemical structure and the liposomal thermosensitivity, which could eventually help develop more efficient or more cost-effective thermoresponsive liposomal carriers. The experiments are corroborated with atomistic computational studies of DPPC:monoalkyl lipid mixtures in an attempt to gain further insight on the phenomenon.[27] The simulations allowed the study of lipid dynamics in the sub-microsecond time scale, demonstrated very good reproduction of experimental results and are also in line with existing theory that increased permeability is the result of lateral area increase of the lipids upon melting and of increased lateral compressibility values.

2. MATERIALS AND METHODS

2.1. Materials. The phospholipids 1,2-dipalmitoyl-*sn*-glycero-3-phosphocholine (DPPC) and 1,2-distearoyl-*sn*-glycero-3-phosphoethanolamine-*N*-[methoxy(polyethylene glycol)-2000] (ammonium salt) (DSPE-PEG) were obtained from Lipoid GmbH (Ludwigshafen, Germany) and Avanti Polar Lipids (Alabaster, AL, USA), respectively. The 1-palmitoyl-2-hydroxy-*sn*-glycero-3-phosphocholine (lyso-PC) was obtained from NOF Co. (Tokyo, Japan), while 1-*O*-hexadecyl-2-acetyl-*sn*-glycero-3-phosphocholine (PAF), 1-*O*-hexadecyl-2-hydroxy-*sn*-glycero-3-phosphocholine (lyso-PAF), and 1-*O*-hexadecyl-2-*O*-methyl-*sn*-glycero-3-phosphocholine (methyl-PAF) were obtained from Sigma Chemicals Co. (St. Louis, MO, USA). 5(6)-Carboxyfluorescein (CF) and Sephadex G-50 (medium) were obtained from Sigma-Aldrich. Nucleopore filters of 100 nm pore size (Whatman) were employed for liposome extrusion.

2.2. Preparation of Thermosensitive Liposomes. For the preparation of thermosensitive liposomes the protocol employed by Mills and Needham has been followed.[16] Small unilamellar liposomes were prepared by the extrusion method[28] employing a laboratory extruder (LiposoFast-Pneumatic, Avestin Inc.).[29] In a typical experiment for preparing a 1 mL dispersion of liposomes, 20.0 mg of DPPC, 3.4 mg of DSPE-PEG (molar ratio of DPPC:DSPE-PEG = 91:4), and the corresponding amounts of monoalkyl phospholipids for the preparation of thermoresponsive liposomes of a molar ratio of 91:4:5 or 91:4:10, were dissolved in a chloroform/methanol solution (2:1 (v/v)) for the formation, in the usual manner, of lipid films.[29] The film was hydrated with 1 mL of a buffer solution composed of PBS (20 mM, pH = 7.4) containing 1 μM of the appropriate monoalkyl phospholipid, and the obtained suspension was extruded through two stacked polycarbonate filters of 100 nm pore size. Twenty-five cycles were applied at 50 °C. CF-loaded liposomal dispersions were prepared following the same as the aforementioned procedure employing CF dissolved in the aqueous phase at a concentration at which its fluorescence is quenched (50 mM, pH 7.4). After extrusion, the non-encapsulated CF was removed by gel size-exclusion column filtration employing Sephadex G-50 columns and the preceding phosphate buffer as an eluent.[16]

2.3. Characterization Techniques. The obtained liposomes were investigated by dynamic light scattering (DLS), ζ-potential experiments, and high-precision differential scanning calorimetry, while the permeability of the bilayer at various temperatures was assessed by monitoring the CF release (see section 2.4).

DOI: 10.1021/acs.jpcb.6b02783
J. Phys. Chem. B XXXX, XXX, XXX−XXX

The size and polydispersity of liposomal dispersions were determined at 22 °C by dynamic light scattering employing an AXIOS-150/EX (Triton, Hellas) apparatus with a 30 mW laser source and an Avalanche photodiode detector at an angle of 90°. For these experiments 100 μL of liposomes was diluted with 0.6 mL of PBS buffer. For each dispersion, 10 scattering measurements were acquired and the results were averaged. Autocorrelation functions were collected for 20 s and analyzed using the CONTIN algorithm to obtain the apparent hydrodynamic radii distribution. The ζ-potential values were obtained at 22 °C using ZetaPlus of Brookhaven Instruments Corp. (Long Island, NY, USA) equipped with a 35 mW solid-state laser emitting at 660 nm. From the determined electrophoretic mobility, the ζ-potential of the liposomal dispersions was calculated using the Smoluchowski equation. In a typical experiment, 200 μL of a liposomal dispersion was diluted with 1.4 mL of PBS buffer and introduced into the instrument cell. Ten measurements were collected for each dispersion, and the results were averaged. The standard deviation of the measurements was less than 1%.

High-precision differential scanning calorimetry experiments were performed using the VP-DSC microcalorimeter (Microcal Inc., Northampton, MA, USA). The main lipid phase transition has been studied for both the PEGylated DPPC:DSPE-PEG liposomes as well as for the liposomes incorporating the four different monoalkyl chain lipids at 5 and 10% molar ratio. Prior to scanning, all of the liposomal dispersions were degassed for about 15 min under vacuum. Heating and cooling scans were carried out from 25 to 60 °C at a rate of 10 K/h. Liposomes were diluted with water in a molar ratio 1:1 before the measurements. The thermodynamic parameters T_m, ΔC_{pmax}, ΔH, and $\Delta T_{1/2}$ were obtained with the built-in Origin software using the data registered during the second and third run which were found to be identical.

2.4. Temperature- and Time-Dependent CF Release. CF release was monitored by continuously registering the fluorescence intensity of dispersions using a Cary Eclipse fluorescence spectrophotometer coupled with a single-cell Peltier accessory (type SPVF 1×0) able to continuously stir and stabilize the temperature in the cell with 0.1 °C precision, both from Varian Inc. (Mulgrave, Victoria, Australia). Typically, 40 μL of prepared liposomes was diluted in 2700 μL of preheated 20 mM PBS buffer solution which was already placed and thermally equilibrated in the fluorescence cell. Upon addition of the liposomal dispersions in the preheated buffer under continuous stirring, the registering of the fluorescence intensity was immediately started. It was thus possible for the liposomes to reach the desired temperature within seconds and to also monitor online the content release over time from the first 10 s after the addition by following the fluorescence intensity of released CF (excitation wavelength = 493 nm; emission wavelength = 513 nm). Release measurements at 37, 38, 39, 40, 41, 42, and 43 °C were performed for 30 min. CF release was calculated as CF (%) = $(I_t - I_o)/(I_{max} - I_o) \times 100$. After 30 min, 150 μL of 10% Triton X-100 was added to the samples in order to calculate I_{max} for each temperature.[16] I_o values of each dispersion were determined at 25 °C in separate experiments conducted as described previously. The temperature dependence of CF release is shown by plotting its percent release after the first 5 min incubation time at the designated temperatures, from 37 to 43 °C. In addition, liposomal stability at 37 °C was assessed by incubating 40 μL of the liposomal dispersions in 2.7 mL of PBS buffer, registering the fluorescence intensity after 24 h and calculating the CF release as described earlier. The leakage rate of liposomal content was proposed to follow first order kinetics,[30] and, thereafter, many research groups[17,31−33] used this supposition to calculate the apparent rate constant, k, of CF, or any other drug, release using the equation $RF(t) = RF_{max}(1 - e^{-kt})$, where RF is the fraction of CF that is released at each time point, t, and RF_{max} the maximum attained RF. The first 2 min of incubation at each temperature were used for the calculation of k, utilizing the fitting algorithms embedded in the Origin software.

2.5. Lipid Bilayer Simulations. A DPPC bilayer comprising 128 lipids was constructed using the CHARMM Membrane Builder GUI.[34] The four mixtures of DPPC with monoalkyl lipids at 0.1 molar fraction were prepared by substituting 12 DPPC molecules (evenly distributed between the two bilayer leaflets) with 12 molecules of lyso-PC, PAF, lyso-PAF, or methyl-PAF. The AMBER v14 package[35] with the latest Lipid14[36] force field and the TIP3P water model,[37] at the hydration level of 30.1 water molecules per lipid which was employed for the development of Lipid14, were used for simulation of the systems. Force field parameters for the monoalkyl lipids were prepared according to the Lipid11 and Lipid14 development philosophy,[38] as detailed in the Supporting Information.

After equilibration of the systems for 50 ns (Supporting Information) three independent production runs of 200 ns for each bilayer system in the isothermal−isobaric (*NPT*) ensemble at 323 K were initiated from different random seeds. Three independent 200 ns runs for each system were also performed at 314 K, which were seeded from the last frame of the equilibrated systems at 323 K. All simulations were performed with the GPU-accelerated version of PMEMD program of AMBER v14,[39] employing the SPFP precision model of Le Grand and Walker.[40] Analysis was conducted on the equilibrated portion of the trajectories using the CPPTRAJ module of AmberTools v15[41] (Supporting Information), and results are presented as block averages (6 × 100 ns) over the triplicate 200 ns *NPT* simulations ± standard deviation.

3. RESULTS

3.1. Liposomal Physicochemical Characteristics. The hydrodynamic radius and polydispersity of liposomal dispersions were studied by DLS. The mean radii of all liposomal dispersions as determined by CONTIN were found to be, within experimental error, $45_{\pm 5}$ nm, consistent with the pore size of the polycarbonate filter employed. The corresponding distributions were different for the two different classes of thermoresponsive polymers: liposome formulations containing 5% monoalkyl lipids had size distributions clearly more sharp compared to those recorded for the formulations containing 10% monoalkyl phospholipids (Figure 1). Taking into consideration that all process variables during extrusion were strictly kept the same, this difference can be attributed to the enhanced fluidity of the liposomal membranes at temperatures above the main lipid transition when increased quantities of single-chain lipids are present in the bilayer.

The ζ-potential values of all formulations were found in all cases to be, within experimental error, the same ($-3.0_{\pm 1.5}$ mV) which was anticipated due to the presence of the same polar groups, i.e., the phosphatidylcholine group, in all lipids employed. The small negative value can be attributed to the presence of DSPE-PEG which bears a negative net charge. Overall, in all the liposomal formulations tested the same mean

DOI: 10.1021/acs.jpcb.6b02783
J. Phys. Chem. B XXXX, XXX, XXX−XXX

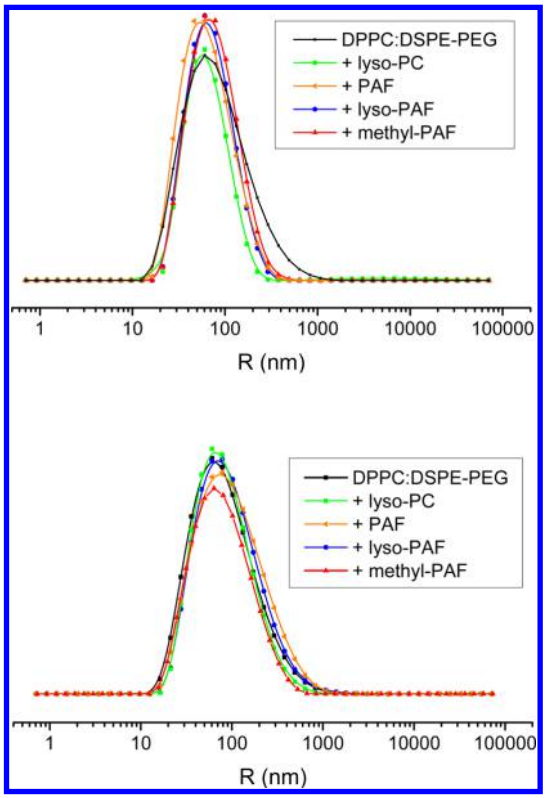

Figure 1. Intensity weighted hydrodynamic radius distributions of DPPC:DSPE-PEG-based thermoresponsive unilamellar liposomes containing 5 mol % (upper part) or 10 mol % (lower part) monoalkyl phospholipids.

size and surface charge is attained giving the additional advantage that any variations in their properties would solely result from the structural characteristics of their lipids.

3.2. Differential Scanning Calorimetry. Differential scanning microcalorimetry (microDSC) provides information on the enthalpy and entropy of transitions and serves as a powerful tool for quality control of unilamellar liposomes, as well as for the rational development of lipidic nanocarriers.[42−44] The thermal behavior of PEGylated DPPC liposomes as well as of the same liposomes containing monoalkyl lipids at 5 and 10 mol % was studied by microDSC at the temperature range from 25 to 60 °C. Their DSC profiles of the second heating run, after a thermal equilibration taking place during the first heating/cooling run,[45] are shown in Figure 2, while the thermodynamic parameters of all formulations are summarized in Table 1. The DSC profiles of the third heating/cooling run are identical with that of the second run in all formulations. For comparison purposes only, the thermodynamic parameters of the first heating run are also tabulated in parentheses (Table 1). For the parent DPPC:DSPE-PEG liposomes the T_m of the main lipid gel to liquid crystalline phase transition ($P_\beta \rightarrow L_\alpha$) is observed at 42 °C as expected for DPPC liposomes.[46] For the main transition of all formulations a single peak was registered in the DSC scans providing evidence that, at least at the concentrations studied, the resulting systems are uniform not involving inhomogeneities within the membrane.[47] As shown in Table 1, T_m is the same for all formulations containing either 5% or 10% monoalkyl ether lipids. As an exception, after taking into consideration the error in the determination of T_m, the only statistically significant difference in T_m is that of liposomes containing methyl-PAF. Liposomes with 5% methyl-PAF

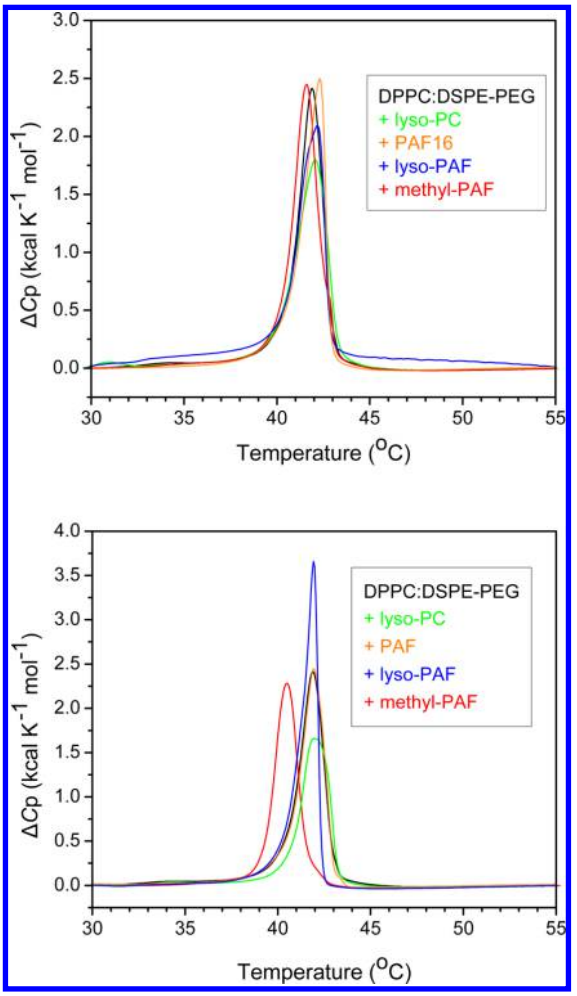

Figure 2. DSC profiles of ΔC_p vs T for the main phase transition of DPPC- and DPPC:DSPE-PEG-based thermoresponsive unilamellar liposomes containing 5 mol % (upper part) or 10 mol % (lower part) monoalkyl phospholipids. The heating scan rate for all of the thermographs was 10 K/h.

exhibit a slight but definite decrease in T_m, and this decrease is more prominent (~1.5 °C) when 10% of this lipid is incorporated in the bilayer. This suggests that methyl-PAF due to the presence of its bulky methyl group in the middle of the glyceryl group disturbs the bilayer order, possibly through the alteration of the van der Waals interactions between neighboring groups.[48−50]

The enthalpies of the main transition registered (Table 1) in formulations containing 5% monoalkyl lipids are only minimally affected, indicating a successful incorporation of these molecules in the gel phase of the bilayer. Increase of their incorporation percentage to 10% resulted in a small but unequivocal decrease of ΔH without, however, particularly affecting molecular cooperativity within the bilayers. Although the differences are small, it is interesting to note that incorporation of lyso-PAF in the bilayer at 5% and 10% concentration results in the highest ΔH values suggesting that this ether lipid with no carbon group at the 2-position of the glycerol moiety favors (at 5%), or disturbs minimally (at 10%), the packing of the gel phase. The observed high cooperativity values of the transition (typically taken as $1/\Delta T_{1/2}$, where $\Delta T_{1/2}$ is the temperature width at half-maximum of the DSC peak) in the presence of this compound is in line with the

DOI: 10.1021/acs.jpcb.6b02783
J. Phys. Chem. B XXXX, XXX, XXX−XXX

Table 1. DSC Parameters (T_m, C_{pmax}, $\Delta T_{1/2}$, and ΔH) of the Main Lipid Phase Transition of DPPC- and DPPC:DSPE-PEG-Based Thermoresponsive Unilamellar Liposomes Obtained during the Second Heating Run[a]

sample (% molar ratio monoalkyl lipid)	T_m (°C)	ΔH (kcal mol^{-1})	$\Delta T_{1/2}$ (°C)
DPPC:DSPE-PEG	$41.9_{\pm 0.2}$ (41.8)	$4.5_{\pm 0.3}$ (4.3)	1.5 (1.4)
DPPC:DSPE-PEG:lyso-PC (5%)	$42.1_{\pm 0.2}$ (42.1)	$4.3_{\pm 0.3}$ (3.8)	1.9 (1.7)
DPPC:DSPE-PEG:PAF (5%)	$42.3_{\pm 0.2}$ (42.4)	$3.9_{\pm 0.3}$ (4.1)	1.4 (1.3)
DPPC:DSPE-PEG:lyso-PAF (5%)	$42.2_{\pm 0.2}$ (42.1)	$4.8_{\pm 0.4}$ (4.7)	1.6 (1.6)
DPPC:DSPE-PEG:methyl-PAF (5%)	$41.6_{\pm 0.2}$ (41.2)	$4.6_{\pm 0.3}$ (4.5)	1.5 (2.5)
DPPC:DSPE-PEG:lyso-PC (10%)	$42.0_{\pm 0.2}$ (41.8)	$3.3_{\pm 0.3}$ (3.2)	1.8 (1.6)
DPPC:DSPE-PEG:PAF (10%)	$42.0_{\pm 0.2}$ (43.0)	$4.0_{\pm 0.3}$ (4.2)	1.4 (1.8)
DPPC:DSPE-PEG:lyso-PAF (10%)	$41.9_{\pm 0.2}$ (41.8)	$4.2_{\pm 0.3}$ (4.4)	1.0 (1.0)
DPPC:DSPE-PEG:methyl-PAF (10%)	$40.4_{\pm 0.2}$ (40.1)	$3.6_{\pm 0.3}$ (3.8)	1.3 (1.0)

[a]For comparison, the parameters obtained during the first heating run are shown in parentheses.

increased ΔH values. This designates a favorable interaction of lyso-PAF with DPPC suggesting a more homogeneous distribution of these lipids in the bilayer and that the local order extends over larger areas in this particular case.[50] In general, all the ether lipids impart small, almost insignificant changes, at 5% incorporation, in the ΔH and $\Delta T_{1/2}$ values in contrast to lyso-PC containing membranes, which exhibit the lowest cooperativity (broader DSC peaks) and ΔH values registered. The differences in the thermodynamic parameters of lyso-PC containing liposomes are most prominent when compared with liposomes containing the corresponding ether derivative, i.e., lyso-PAF. Overall, the thermodynamic parameters of liposomes containing monoalkyl ether lipids are comparable to those of DPPC:DSPE-PEG liposomes. Given that the transition temperatures and cooperative unit sizes of ether lipids containing bilayers are comparable to those of DPPC bilayers, and that the ether lipids do not melt independently (no extra peak in their DSC profiles is observed), it is reasonable to propose, given the similarity of the polar part of the molecules and of the aliphatic chain length, that the monoalkyl lipids dissolve in the DPPC bilayer and mix randomly (ideally) both in the gel and in the fluid phase.[51]

3.3. Time-Dependent CF Release. Time-dependent CF release from liposomes containing 5% or 10% monoalkyl lipids was continuously monitored online for 30 min. This time frame is justified given that, in practice, hyperthermia treatments are exercised for approximately 0.5 h after administration of drugs or drug-loaded liposomes.[9,33,52] All samples are stable at 37 °C having a maximum CF leakage of approximately 7% after 30 min incubation (Supporting Information Figure S1) while most of the CF is leaking within the first 10 min. The registered profiles of lyso-PC are consistent with the corresponding profiles of similar formulations reported in the literature. For instance, an ~10% CF release was reported for DPPC:DSPE-PEG:lyso-PC (84:4:10) within 30 min, with most of the release being observed within the first 10−15 min.[16] The release profiles for the different formulations studied do not differentiate substantially although it is clear that control DPPC:DSPE-PEG liposomes have the slowest release, which is expected since no monoalkyl lipids are embedded in the bilayer. For the thermosensitive preparations, the observed release is higher for liposomes containing either 5% or 10% methyl-PAF, although the difference with the standard lyso-PC thermosensitive liposomes is not statistically significant especially when 10% molar ratio of these lipids is employed. The percentage release of CF after 24 h incubation time at 37 °C is also typically studied for thermoresponsive liposomes, and the results are presented in Supporting Information (Table S1). Again no substantial differentiation in the released CF is observed for all formulations studied. While control liposomes definitely appear more stable, the effect of various monoalkyl lipids on the stability of liposomes is marginally in favor of lyso-PC formulations compared to the ether lipids.

On the other hand at 41 °C, i.e., close to the T_m, and at the temperature practically encountered during mild hyperthermia therapy, the corresponding profiles (Figure 3) show a rapid release of CF, which almost reaches its maximum in each sample within the first 5 min, and in most of the cases even sooner (approximately within 2 min). The obtained results of CF release from control samples are in accordance with already published data although small variations in the release profiles

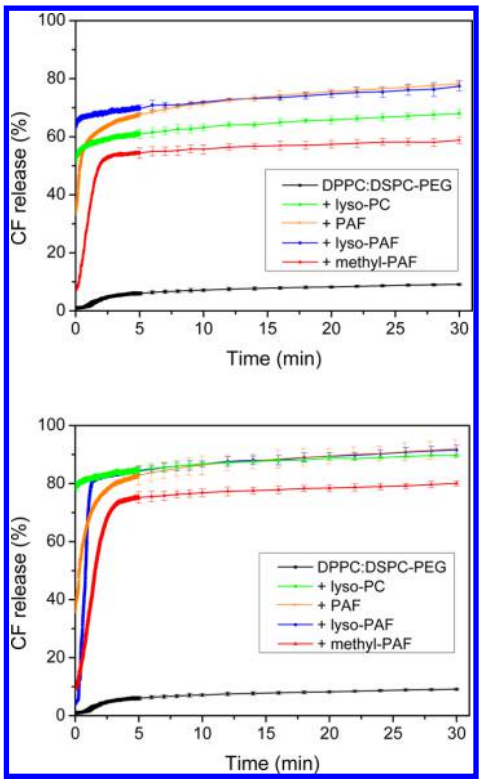

Figure 3. Time-dependent CF release at 41 °C from DPPC:DSPE-PEG-based thermoresponsive unilamellar liposomes containing 5 mol % (upper part) or 10 mol % (lower part) monoalkyl phospholipids. Measurements were taken every 0.2 s during the first 5 min of the incubation period, every 1 min until 10 min, and every 2 min afterward. For clarity, error bars are shown only after the first 5 min period.

DOI: 10.1021/acs.jpcb.6b02783
J. Phys. Chem. B XXXX, XXX, XXX−XXX

are to be expected due to differences in the preparation protocol or of their size.[53] Thus, it has been reported that liposomes consisting of DPPC:DSPE-PEG (90:4) have an ~10% release of CF after 5 min incubation time at 41 °C, while the "standard" thermosensitive liposomes consisting of DPPC:DSPE-PEG:lyso-PC (90:4:10) have a reported $85_{\pm 8}$% release at 40.9 °C.[17] Consistent with the above, in the work of Sandström et al., CF release from DPPC:DSPE-PEG:lyso-PC18 (90:4:10) liposomes was 50.9% and 84.5% after heating at 41.5 °C for 1 and 30 min, respectively.[15]

Comparing the time-dependent CF release measurements from liposomes containing ether monoalkyl lipids to that of the ester counterpart lyso-PC, it is clear that at 10% incorporation (which is used in the standard thermoresponsive liposomes) all formulations behave identically, releasing most of their content within the first 5 min and reaching an almost constant value of ~90% after 30 min (see also Table 2). As an exception, methyl-

Table 2. Apparent Release Rate Constants of CF from Thermoresponsive Liposomes Incubated at 41°C and Total CF Release at the Same Temperature within the First 30 min[a]

liposome formulation	k[b] (s^{-1})	total CF release (%)
DPPC:DSPE-PEG	$0.72_{\pm 0.03}$	$9.1_{\pm 0.1}$
DPPC:DSPE-PEG:lyso-PC 5%	$2.75_{\pm 0.15}$	$68.0_{\pm 0.5}$
DPPC:DSPE-PEG:PAF 5%	$(2.40_{\pm 0.10})$	$78.1_{\pm 0.9}$
DPPC:DSPE-PEG:lyso-PAF 5%	(3.75 ± 0.25)	$75.5_{\pm 1.0}$
DPPC:DSPE-PEG:methyl-PAF 5%	0.82 ± 0.03	$58.8_{\pm 0.5}$
DPPC:DSPE-PEG:lyso-PC 10%	$(2.50_{\pm 0.15})$	$89.6_{\pm 1.0}$
DPPC:DSPE-PEG:PAF 10%	$1.25_{\pm 0.12}$	$92.0_{\pm 1.0}$
DPPC:DSPE-PEG:lyso-PAF 10%	$5.80_{\pm 0.20}$	$91.6_{\pm 1.6}$
DPPC:DSPE-PEG:methyl-PAF 10%	$0.90_{\pm 0.03}$	$80.0_{\pm 0.9}$

[a]The first 2 min of release profiles were used for the calculation of k, the apparent rate constant. [b]Values in parentheses are underestimations of the actual values anticipated at the initial time period (see text).

PAF containing liposomes exhibit a slower release rate and lower final release percentage after 30 min (80%). On the other hand, liposomes containing only 5% monoalkyl lipids have different release profiles and in this case a structure−property relationship can be tentatively formed. As mentioned earlier, methyl-PAF has the lowest release properties demonstrating the unfavorable effect of the methyl group at the 2-position of the glycerol moiety. However, both PAF and lyso-PAF ether lipids induce higher CF release than lyso-PC, signifying the role of the ether bond at the 1-position of the glycerol moiety. For these thermosensitive liposomes the total release registered is 75−78%, which is 10% higher than that of lyso-PC and only 10% less than the release obtained from liposomes containing twice the amount of monoalkyl lipids.

The observed differences are also reflected in the apparent rate constants, k, that are calculated from the experimental data, as described in the experimental section, and included in Table 2. It should be emphasized that it was not possible to accurately fit the entire release profile, because as time progresses the release becomes significantly slower reaching plateau values and practically minimizing the rate constants. Therefore, the first 2 min of release profiles were used for the calculation of k. Also, given that for certain formulations even the first registered value (taken within less than 10 s after bringing the liposomes at 41 °C) is very high (close to 60 or even 80%), the initial rate constant is practically not possible to be determined and the tabulated apparent rate constant is underestimated.

3.4. Temperature-Dependent CF Release. In order to examine the temperature dependence of CF release, the corresponding profiles of all liposomal formulations at 37−43 °C were experimentally determined (see Supporting Information, Figures S2−S10). In order to facilitate comparison, the CF release values after 5 min incubation time at each temperature and for every formulation tested are shown in Figure 4. It is

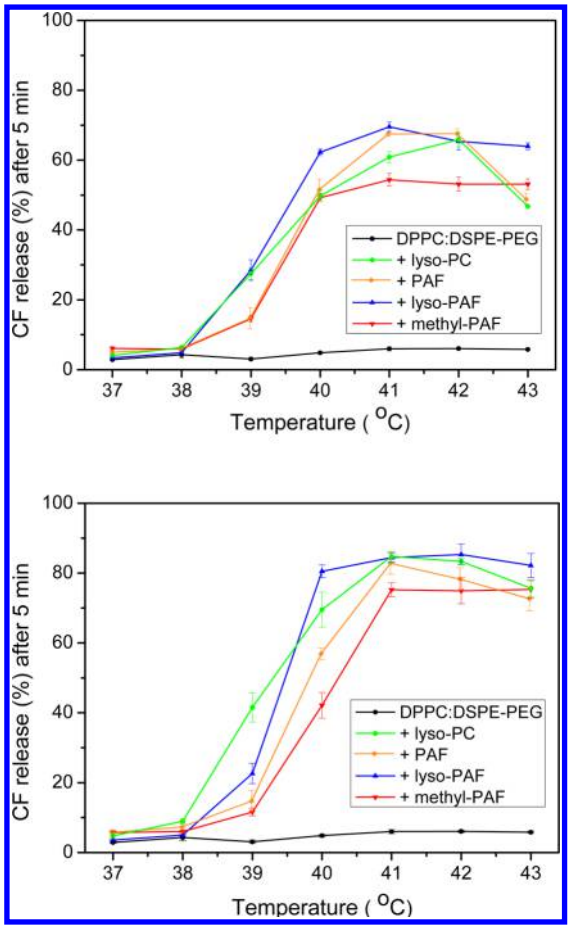

Figure 4. CF release from DPPC:DSPE-PEG-based thermoresponsive unilamellar liposomes containing 5 mol % (upper part), or 10 mol % (lower part) monoalkyl phospholipids, measured after the first 5 min period of incubation time at various temperatures, from 37 to 43 °C.

clear that all samples are quite stable at temperatures up to 38 °C and become progressively permeable at temperatures close to T_m. For liposomes containing 5% monoalkyl lipids substantial CF release is observed at 40 °C which maximizes at 41−42 °C, i.e., at the gel to liquid crystalline transition temperature of liposomes. Further increasing the temperature, a noticeable decline is observed as it is typical for other thermosensitive liposomal formulations.[4,6,16,17] As previously shown, the methyl-PAF liposomes exhibit the lowest, while lyso-PAF and PAF liposomes the highest release values. Liposomes containing 10% monoalkyl lipids display higher release values but on the other hand the CF release at 38 and 39 °C is significant, especially for the lyso-PC formulation. Indeed, the value obtained at 39 °C (~40%) is in excellent agreement with that reported in the literature for DPPC:DSPE-PEG:lyso-PC (86:4:10) liposomes.[16] On the contrary, ether-

DOI: 10.1021/acs.jpcb.6b02783
J. Phys. Chem. B XXXX, XXX, XXX−XXX

Table 3. Average Properties (±Standard Deviation) over Three Independent 200 ns Simulations of Pure DPPC and the Four DPPC:Monoalkyl Lipid (10 mol %) Systems in the *NPT* Ensemble at 323 K[a]

			bilayer thickness			
lipid system at 323 K	A_L (Å^2)	V_L (Å^3)	h_L (Å)	D_{HH} (Å)	K_A (mN/m)	D_{xy} (10^{-8} cm^2/s)
Experiment	63.1[57] 64.3[58]	1232[59]	38[60] 38.3[59] 39.0[57]		231[59]	12.5[61] 15.2[62]
DPPC	$62.6_{\pm0.4}$	$1174_{\pm0.8}$	$37.5_{\pm0.2}$	$38.8_{\pm0.5}$	$245_{\pm61}$	$11.0_{\pm0.7}$
DPPC:lyso-PC	$66.0_{\pm0.2}$	$1124_{\pm0.5}$	$34.0_{\pm0.1}$	$36.2_{\pm0.4}$	$281_{\pm38}$	$13.0_{\pm0.9}$)
DPPC:PAF	$67.8_{\pm0.3}$	$1131_{\pm0.5}$	$33.4_{\pm0.1}$	$35.8_{\pm0.4}$	$274_{\pm68}$	$12.9_{\pm1.3}$
DPPC:lyso-PAF	$66.1_{\pm0.3}$	$1124_{\pm0.4}$	$34.0_{\pm0.2}$	$36.4_{\pm0.4}$	$270_{\pm33}$	$11.7_{\pm1.4}$
DPPC:methyl-PAF	$66.9_{\pm0.2}$	$1128_{\pm0.4}$	$33.7_{\pm0.1}$	$36.2_{\pm0.4}$	$280_{\pm42}$	$12.5_{\pm1.5}$

[a]Experimental properties are taken from measurements at 323 K. Bilayer thickness is given as the average lipid thickness, h_L, and peak-to-peak headgroup distance, D_{HH}, calculated from the electron density profiles. The lateral diffusion coefficient, D_{xy}, was estimated from the *NPT* simulations. A_L = area-per-lipid, V_L = volume-per-lipid , K_A = isothermal area compressibility modulus, and D_{xy} = lateral diffusion coefficient.

based formulations proved to be more stable at this temperature (~25% release for lyso-PAF, ~15% for PAF) which suggest that these formulations are more stable in lower temperatures than the commonly used lyso-PC-based formulation.

Overall all formulations have their maximum release values at temperatures close to the T_m and their release properties are comparable at 10% incorporation. Membrane permeabilities at the T_m differ in favor of the ether lipids PAF and lyso-PAF only when a lower, 5 mol %, incorporation is employed while they are more stable at temperatures less than 39 °C which is an additional advantage in mild hyperthermia treatments.

3.5. Molecular Dynamics Simulations of DPPC:Monoalkyl Lipid Bilayers. Atomic level computer simulations have increased our understanding of the properties of biological membranes and have evolved as a complementary technique in the study of bilayers.[54,55] Recent studies have been focused on more complicated and realistic systems consisting of mixtures of lipids with molecules of biological interest, such as cholesterol.[56] To this end, we employed all-atom molecular dynamics simulations of model systems comprising 128 DPPC lipids or 128 DPPC:monoalkyl lipid mixtures at 10% molar fraction. The latest AMBER force field, Lipid14,[36] which has been shown to reproduce fairly good a range of thermodynamic and dynamic properties for a number of simple lipids without applying a surface tension, was further refined to account for the different headgroups of the selected monoalkyl lipids (Supporting Information). Taking advantage of the GPU implementation of AMBER,[39,40] we performed molecular dynamics in the isothermal−isobaric ensemble (*NPT*) at temperatures of 323 and 314 K for a total of more than 6 μs simulation time. The simulations of pure DPPC at 323 K were first performed and served as reference with respect to available experimental data so as to verify our simulation protocol and to fine-tune the Lipid14 force field for the simulation of the monoalkyl chain lipids. Subsequently, the simulations at 314 K were seeded from the equilibrated systems at 323 K that sampled the liquid crystalline phase.

The properties of DPPC calculated from our data (Table 3) are in excellent agreement with the results obtained by the developers of Lipid14 force field[36] and are in good agreement with experimental data.[57−62] In particular, the bilayer surface area per DPPC lipid (A_L) reported is within 3% of the experimental value of 63−64 Å^2, which can be safely considered an indication that the simulations sample the correct liquid crystalline phase (L_α). The volume per lipid (V_L) is underestimated by less than 5% of the experimental value, and the bilayer thickness calculated from the electron density profiles as the peak-to-peak headgroup distance, D_{HH}, is well within the experimental range of 38−39 Å (Table 3). Calculation of the electron density profile of DPPC at 323 K (Supporting Information Figure S12) exhibits the characteristic symmetrical profile with water penetrating up to the carbonyl groups in agreement with experimental findings.[58,60] The isothermal area compressibility modulus, K_A, calculated from the fluctuation in the surface area of the lipids, (Supporting Information) falls close to the experimental value and within the standard deviation of the simulations, which is quite high as a result of the high variance observed in the values of A_L (Table 3 and Supporting Information Figure S11). Perhaps the most informative parameter characterizing the ordering of the lipid acyl tails is the NMR order parameter S_{CD}, a measure of the relative orientation of the C−H(D) bonds with respect to the bilayer normal. The calculated $|S_{CD}|$ order parameter for the *sn*1 and *sn*2 chains of DPPC at 323 K (Supporting Information Figure S16) are in very good agreement with NMR experiments, as noted also in the development of the Lipid14 force field.[36] Considering the dynamic lipid properties, we calculated the lipid lateral diffusion coefficient, D_{xy}, using the Einstein relation as described in the Supporting Information. The calculated values (Table 3), albeit underestimated, are on the same order of magnitude as experimental data, which were obtained by several different methods exhibiting a wide range of values in the literature.[63]

Examination of the structural properties obtained for the four DPPC:monoalkyl lipid models at 323 K reveals a statistically significant increase in the average area-per-lipid A_L by 5−8% (3−5 Å^2) with respect to pure DPPC (Table 3). Accordingly, we observed a decrease in the calculated volume-per-lipid V_L by 4% (43−50 Å^3) and in the average bilayer thickness D_{HH} by 6−8% (2.4−3.0 Å). The decrease of the bilayer thickness is illustrated in Figure 5A by comparing the calculated electron density profiles of the phosphate groups in pure DPPC and DPPC:PAF bilayers. More interestingly, comparison of the corresponding water electron density profiles indicates that the solvent penetrates deeper into the DPPC:PAF bilayer by approximately 3 Å in each side (Figure 5A), which is also the case for all four DPPC:monoalkyl lipid systems examined (Supporting Information Figures S12 and S13). This effect can be rationalized with regard to the ordering of the lipids in the bilayer, which is expected to be lower in the case of monoalkyl lipids. In fact, comparison of the calculated order parameters for the alkyl chain of the four monoalkyl lipids and the *sn*1 chain of DPPC indicates that the monoalkyl chains, and in particular of

DOI: 10.1021/acs.jpcb.6b02783
J. Phys. Chem. B XXXX, XXX, XXX−XXX

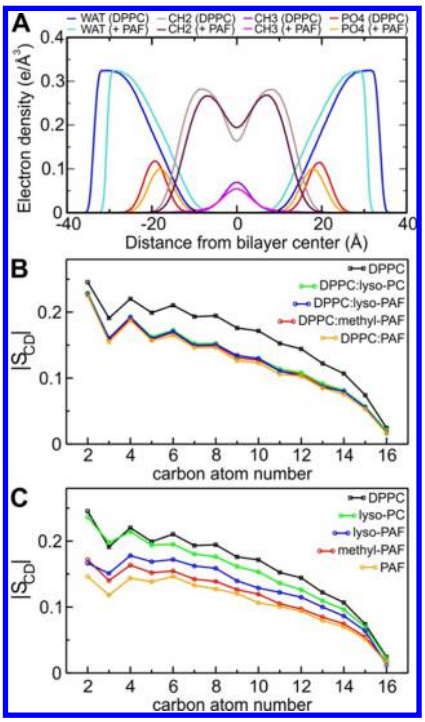

Figure 5. (A) Selected components of the electron density profiles of pure DPPC in comparison to DPPC:10 mol % PAF. The total electron density profiles calculated from the *NPT* simulations at 323 K were decomposed into contributions from the water (WAT), phosphate (PO4), methylene (CH2), and terminal methyl groups (CH3). (B) Comparison of the $|S_{CD}|$ order parameters of DPPC *sn*1 chain between the pure DPPC and the four DPPC:monoalkyl lipid systems at 323 K. (C) $|S_{CD}|$ order parameters of the *sn*1 chain of pure DPPC and of the alkyl chain of the four monoalkyl lipids averaged over the simulations at 323 K.

methyl-PAF and PAF, are less ordered than DPPC and lyso-PC (Figure 5C). The lower degree of ordering in the mixtures of DPPC with the four monoalkyl lipids results in the decrease of the $|S_{CD}|$ order parameters of both *sn*1 and *sn*2 chains of the DPPC lipids accordingly (Supporting Information Figure S16). However, the effect of the different monoalkyl lipids on the ordering of DPPC acyl chains is not as clear as calculated for the monoalkyl lipids (Figure 5B), albeit following the same trend shown in Figure 5C. The calculated lateral diffusion coefficients of the four mixtures exhibit a systematic increase with respect to pure DPPC (Table 3), although this should be considered tentatively as the observed differences fall within the standard deviation of the approach employed.

Since our experimental data were obtained at temperatures close to the T_m value (41 °C), we performed also simulations of the same lipid models at 314 K seeded from the equilibrated systems at 323 K. Pure DPPC simulations at 314 K yielded structural properties that are characteristic of a fluid-to-gel transition, as demonstrated by the decrease of the average area-per-lipid from ∼63 to 52 Å^2 and the increase of the head-to-head bilayer thickness to 47 Å (Table 4). Typical structural properties of DPPC at the gel phase that were extracted from experiments at 20 °C are D_{HH} = 44.2 Å, A_L = 47.9 Å^2, and V_L = 1144 Å^3.[59] The observed transition takes place within the initial 50 ns simulation from 323 to 314 K and displays a well-equilibrated trajectory after 100 ns (see A_L as a function of simulation time in Supporting Information Figure S11). Similar results were obtained by performing equilibration and production molecular dynamics of pure DPPC models at 314 K (data not shown). The transition effect on the DPPC lipids can be illustrated by the electron density profile and its decomposition into contributions from the different groups (Figure 6A and Supporting Information Figures S14 and S15). In addition, the calculated order parameter $|S_{CD}|$ of the DPPC *sn*1 chain exhibit significantly higher values (ordering) with respect to the corresponding values at 323 K, an effect that is apparent up to C-14 of the alkyl chain (Figure 6B,C and Supporting Information Figure S17). As a consequence, the compressibility modulus K_A of DPPC at 314 K increases dramatically and the lateral diffusion coefficient decreases by 5-fold (Table 4).

In sharp contrast, the simulations of the four DPPC:monoalkyl lipid mixtures at 314 K exhibit characteristic properties of the L_α phase (Table 4 and Figure 6A), albeit influenced by the drop in temperature. In particular, A_L and V_L values at 314 K display a decrease of 2−3%, and D_{HH} increase by 1−2% with respect to properties calculated at 324 K. Similarly, the calculated K_A modulus and the D_{xy} coefficient exhibit lower values, although these data cannot be safely interpreted as mentioned earlier. Still, our simulations at 314 K indicate that the presence of the monoalkyl lipids decrease the ordering of the DPPC lipids as demonstrated by the calculated S_{CD} values of the DPPC acyl chains in the DPPC:monoalkyl lipid mixtures (Figure 6B and Supporting Information Figure S17). In addition, as evident from the water electron density profiles of the DPPC:monoalkyl systems at 314 K, solvent molecules penetrate deeper in each side of the bilayer by ∼3 Å in comparison to pure DPPC (Figure 6A and Supporting Information Figure S15). Although a clear conclusion about the effect of the different monoalkyl lipids used in this study cannot be drawn, comparison of the area-per-lipid and order

Table 4. Average Properties (±Standard Deviation) over Three Independent 200 ns Simulations of Pure DPPC and the Four DPPC:Monoalkyl Lipid Systems (10 mol %) in the *NPT* Ensemble at 314 K[a]

			bilayer thickness			
lipid systems at 314 K ($\Delta_{314-323}$)	A_L (Å^2)	V_L (Å^3)	h_L (Å)	D_{HH} (Å)	K_A (mN/m)	D_{xy} (10^{-8} cm^2/s)
DPPC	$52.0_{\pm0.5}$ (−10.6)	$1111_{\pm4.9}$ (−63)	$42.8_{\pm0.2}$ (5.3)	$47.1_{\pm0.9}$ (8.3)	$489_{\pm22}$ (244)	$2.2_{\pm0.6}$ (−8.5)
DPPC:lyso-PC	$64.2_{\pm0.9}$ (−1.8)	$1105_{\pm2.1}$ (−19)	$34.5_{\pm0.4}$ (0.5)	$36.9_{\pm0.6}$ (0.7)	$220_{\pm77}$ (−61)	$10.2_{\pm1.4}$ (−2.8)
DPPC:PAF	$66.3_{\pm0.3}$ (−1.5)	$1113_{\pm0.4}$ (−18)	$33.6_{\pm0.1}$ (0.2)	$36.1_{\pm0.4}$ (0.3)	$254_{\pm24}$ (−20)	$10.2_{\pm1.4}$ (−2.7)
DPPC:lyso-PAF	$64.2_{\pm0.5}$ (−1.9)	$1105_{\pm1.4}$ (−19)	$34.4_{\pm0.3}$ (0.4)	$37.2_{\pm0.7}$ (0.8)	$214_{\pm48}$ (−56)	$10.6_{\pm2.4}$ (−1.1)
DPPC:methyl-PAF	$65.3_{\pm0.3}$ (−1.6)	$1110_{\pm1.0}$ (−18)	$34.0_{\pm0.1}$ (0.3)	$36.4_{\pm0.4}$ (0.2)	$238_{\pm45}$ (−42)	$9.5_{\pm1.3}$ (−3.0)

[a]For DPPC only, the average properties are calculated from the last 100 ns of the equilibrated trajectories; values in parentheses indicate the difference from the corresponding properties at 323 K. A_L = area-per-lipid, V_L = volume-per-lipid, K_A = isothermal area compressibility modulus, and D_{xy} = lateral diffusion coefficient.

DOI: 10.1021/acs.jpcb.6b02783
J. Phys. Chem. B XXXX, XXX, XXX−XXX

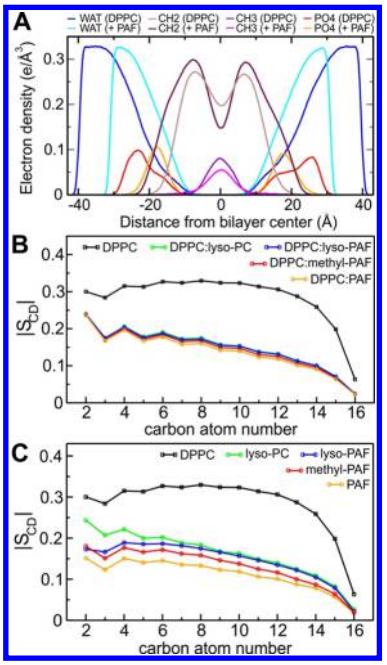

Figure 6. (A) Selected components of the electron density profiles of pure DPPC in comparison to DPPC:10 mol % PAF. The total electron density profiles calculated from the *NPT* simulations at 314 K were decomposed into contributions from the water (WAT), phosphate (PO4), methylene (CH2), and terminal methyl groups (CH3). (B) Comparison of the $|S_{CD}|$ order parameters of DPPC *sn*1 chain between the pure DPPC and the four DPPC:monoalkyl lipid systems at 314 K. (C) $|S_{CD}|$ order parameters of the *sn*1 chain of pure DPPC and of the single alkyl chain of the four monoalkyl lipids averaged over the simulations at 314 K.

parameters obtained at both temperatures suggests that the PAF derivatives exert a more significant effect on bilayer thermosensitivity than lyso-PC.

4. DISCUSSION

To date, lysolipids are the main group of molecules used in the development of temperature-sensitive liposomes. Incorporation of a small amount (typically 10%) of these monoalkyl chain lipids results in an enhancement in the permeability of water-soluble compounds at temperatures in the vicinity of the gel to liquid crystalline main phase transition. The most widely accepted explanation is that of pore formation at the boundaries of liquid and solid domains during the melting process.[15,51,52,64−67] Pore formation is conceivable due to density fluctuations taking place during the transition, and these fluctuations are the result of lateral area increase of the lipids upon melting, typically by ca. 25%.[51] The area-per-molecule significantly changes due to phase transformation, and this is directly associated with increased lateral compressibility values.[68,69] In the present study, all monoalkyl lipids tested impart significant thermoresponsive properties in the DPPC bilayers. Molecular dynamics simulations indicate the increase of area-per-lipid and disordering of the DPPC acyl chains upon incorporation of monoalkyl lipids at 10% molar fraction. Considering the simulations at 323 K where all bilayers are in the fluid phase, the A_L of DPPC mixtures shows an increase of 5−8% and the lateral diffusion coefficients of the DPPC:monoalkyl lipid systems are also higher by 6−18% (Table 3). Interestingly, examination of the decomposed electron density profiles reveals that water penetrates deeper inside the bilayer of the DPPC:monoalkyl chain compositions with respect to pure DPPC (Figure 6A) which will facilitate the transport of water-soluble molecules through the bilayer. Evidently, the presence of single-chain phospholipid is the major characteristic of a molecule that increases the permeability of the membrane during the melting transition.

Less significant than the above, but still important, is the attachment of the alkyl chain through an ether bond, as in PAF and its derivatives, compared to the ester bond that is present in the widely used lyso-PC. It has been concluded[26] by ^{31}P NMR and Raman studies that due to the double-bond character of the ester bond between the O atom and the first C atom of the alkyl chain in lyso-PC, the rotation about this O−C bond axis is hindered and the sterically allowed conformational states for the structural element located in the interfacial region between the polar headgroup and the hydrocarbon region in the bilayer are limited. On the other hand, the corresponding structural element in the ether-linked lyso-PAF has more rotational freedom, and the sterically allowed orientational states are also greater in the interfacial region due to the lack of a bulky carbonyl group. This structural difference is manifested in the observed higher permeability of lyso-PAF liposomes as well as in the cooperativity of the transition which is significantly reduced for lyso-PC liposomes. It is also interesting to note that our molecular dynamics data support this notion by demonstrating that the calculated order parameter $|S_{CD}|$ of the monoalkyl chain of lyso-PC displays significantly higher values with respect to lyso-PAF at 323 K (Figure 6C), and at least for the C-2 to C-4 methylene groups at 314 K (Figure 6C).

Finally, the presence of different groups at the 2-position of the glycerol unit has a minor effect on the permeability of the bilayer. Both molecular dynamic simulations and experiment, within the corresponding errors, show that it is not possible to clearly identify differences in the release properties between the different formulations. In fact, the structural and dynamic properties calculated from the simulations at either temperature exhibit statistically minor differences between the DPPC:monoalkyl lipid bilayers. However, while both PAF and lyso-PAF have the same effect on bilayer properties, methyl-PAF is less effective in inducing thermoresponsive properties. This can be tentatively attributed to the presence of the O−CH_3 group which alters, in an unfavorable way, the packing of the gel phase as indicated both by the low-ΔH value and the significant reduction of T_m (highest among all derivatives).

5. CONCLUSIONS

The presented work supports the general notion that the presence of monoalkyl chain phosphatidylcholines impart thermoresponsive properties in liposomes and further provide evidence that attachment of the long aliphatic chain in the glycerophosphocholine polar group through an ether bond can be beneficial. Taken together, our results suggest that incorporation of the monoalkyl lipids into DPPC liposomes leads to more fluid bilayers with structural and dynamic properties that lead to penetrable membranes near the T_m. From a pharmacological point of view, it is known that lysophosphatidylcholines in general and especially PAF, display important pathophysiological activities and are involved in the pathogenesis of inflammatory diseases.[70,71] However, the inflammatory action of PAF is abolished upon hydrolysis of the acetyl residue at the 2-position and, therefore, lyso-PAF as well as its synthetic analogue methyl-PAF are considered to be

DOI: 10.1021/acs.jpcb.6b02783
J. Phys. Chem. B XXXX, XXX, XXX−XXX

biologically inactive.[72] In addition, methyl-PAF has high metabolic stability and different metabolic effects including inhibition of tumor growth especially studied for the C-18 analogue.[73] Our experiments show that PAF and lyso-PAF at 5 mol % incorporation ratio exhibit more favorable release properties than the commonly used DPPC:lyso-PC formulation, whereas methyl-PAF displayed the lowest release properties. Based on the above, lyso-PAF could be a promising candidate to be utilized in thermoresponsive liposomal formulations since it is a naturally occurring lipid and does not impart adverse pathological effects, while its liposomal formulations show improved stability at temperatures below 39 °C and have better release properties than lyso-PC at low (5%) incorporation ratios.

■ ASSOCIATED CONTENT

Supporting Information

The Supporting Information is available free of charge on the ACS Publications website at DOI: 10.1021/acs.jpcb.6b02783.

Time- and temperature-dependent CF release profiles at 37−43 °C of all liposomal formulations (Figures S1−S10), total CF release from liposomes after 24 h incubation at 37 °C (Table S1), details of the computational methods used for the parametrization of the Lipid14 force field for the monoalkyl lipids, the equilibration and production molecular dynamics, and the calculation of the structural and dynamic properties of the lipids, area-per-lipid (A_L) as a function of simulation time at 323 and 314 K (Figure S11), electron density profiles of DPPC and its mixtures at 323 K (Figures S12 and S13) and 314 K (Figures S14 and S15), $|S_{CD}|$ order parameters of the *sn*1 and *sn*2 acyl chains of DPPC at 323 K (Figure S16) and 314 K (Figure S17), mean square displacement (MSD) curves versus time (Figure S18), and lipid lateral diffusion coefficients calculated from the *NPT* and *NVE* simulations in comparison to the experimental values at 323 K (Table S2) (PDF)

■ AUTHOR INFORMATION

Corresponding Author

*Phone: +30 210 6503616. Fax: +30 210 6511766. E-mail: dtsiourvas@teemail.gr; d.tsiourvas@inn.demokrtios.gr.

Notes

The authors declare no competing financial interest.

■ REFERENCES

(1) Song, C. W. Effect of Local Hyperthermia on Blood Flow and Microenvironment: A Review. *Cancer Res.* **1984**, *44*, 4721s−4730s.

(2) Grüll, H.; Langereis, S. Hyperthermia-Triggered Drug Delivery from Temperature-Sensitive Liposomes Using MRI-Guided High Intensity Focused Ultrasound. *J. Controlled Release* **2012**, *161*, 317−327.

(3) Felice, B.; Prabhakaran, M. P.; Rodríguez, A. P.; Ramakrishna, S. Drug Delivery Vehicles on a Nano-engineering Perspective. *Mater. Sci. Eng., C* **2014**, *41*, 178−195.

(4) Papahadjopoulos, D.; Jacobson, K.; Nir, S.; Isac, T. Phase Transitions In Phospholipid Vesicles. Fluorescence Polarization and Permeability Nieasurenients Concerning the Effects of Temperature and Cholesterol. *Biochim. Biophys. Acta, Biomembr.* **1973**, *311*, 330−348.

(5) Gaber, M. H.; Hong, K.; Huang, S. K.; Papahadjopoulos, D. Thermosensitive Sterically Stabilized Liposomes: Formulation and in Vitro Studies on Mechanism of Doxorubicin Release by Bovine Serum and Human Plasma. *Pharm. Res.* **1995**, *12*, 1407−1416.

(6) Yatvin, M. B.; Weinstein, J. N.; Dennis, W. H.; Blumenthal, R. Design of Liposomes for Enhanced Local Release of Drugs by Hyperthermia. *Science* **1978**, *202*, 1290−1293.

(7) Chelvi, T. P.; Ralhan, R. Designing of Thermosensitive Liposomes from Natural Lipids for Multimodality Cancer Therapy. *Int. J. Hyperthermia* **1995**, *11*, 685−695.

(8) Anyarambhatla, G. R.; Needham, D. Enhancement of the Phase Transition Permeability of DPPC Liposomes by Incorporation of MPPC: A New Temperature-Sensitive Liposome for Use with Mild Hyperthermia. *J. Liposome Res.* **1999**, *9*, 491−506.

(9) Needham, D.; Anyarambhatla, G. R.; Kong, G.; Dewhirst, M. W. A New Temperature-Sensitive Liposome for Use with Mild Hyperthermia: Characterization and Testing in a Human Tumor Xenograft Model. *Cancer Res.* **2000**, *60*, 1197−1201.

(10) Needham, D.; Dewhirst, M. W. The Development and Testing of a New Temperature-Sensitive Drug Delivery System for the Treatment of Solid Tumors. *Adv. Drug Delivery Rev.* **2001**, *53*, 285−305.

(11) Li, L.; ten Hagen, T. L. M.; Schipper, D.; Wijnberg, T. M.; van Rhoon, G.; Eggermont, A. M. M.; Lindner, L. H.; Koning, G. A. Triggered Content Release from Optimized Stealth Thermosensitive Liposomes Using Mild Hyperthermia. *J. Controlled Release* **2010**, *143*, 274−279.

(12) Movahedi, F.; Hu, R. G.; Becker, D. L.; Xu, C. Stimuli-Responsive Liposomes for the Delivery of Nucleic Acid Therapeutics. *Nanomedicine* **2015**, *11*, 1575−1584.

(13) Viard, M.; Puri, A. Stimuli-Sensitive Liposomes: Lipids as Gateways for Cargo Release. *Adv. Planar Lipid Bilayers Liposomes* **2015**, *22*, 1−41.

(14) Ta, T.; Porter, T. M. Thermosensitive Liposomes for Localized Delivery and Triggered Release of Chemotherapy. *J. Controlled Release* **2013**, *169*, 112−125.

(15) Sandström, M. C.; Ickenstein, L. M.; Mayer, L. D.; Edwards, K. Effects of Lipid Segregation and Lysolipid Dissociation on Drug Release from Thermosensitive Liposomes. *J. Controlled Release* **2005**, *107*, 131−142.

(16) Mills, J. K.; Needham, D. The Materials Engineering of Temperature-Sensitive Liposomes. *Methods Enzymol.* **2004**, *387*, 82−113.

(17) Hossann, M.; Wiggenhorn, M.; Schwerdt, A.; Wachholz, K.; Teichert, N.; Eibl, H.; Issels, R. D.; Lindner, L. H. In Vitro Stability and Content Release Properties of Phosphatidylglyceroglycerol Containing Thermosensitive Liposomes. *Biochim. Biophys. Acta, Biomembr.* **2007**, *1768*, 2491−2499.

(18) Lindner, L. H.; Eichhorn, M. E.; Eibl, H.; Teichert, N.; Schmitt-Sody, M.; Issels, R. D.; Dellian, M. Novel Temperature-Sensitive Liposomes with Prolonged Circulation Time. *Clin. Cancer Res.* **2004**, *10*, 2168−2178.

(19) Hashizaki, K.; Taguchi, H.; Tsuchiya, K.; Sakai, H.; Abe, M.; Saito, Y.; Ogawa, N. Calorimetry and Cryo-transmission Electron Microscopic Studies of PEG2000-Grafted Liposomes. *Chem. Pharm. Bull.* **2006**, *54*, 561−563.

(20) Tagami, T.; Ernsting, M. J.; Li, S.-D. Optimization Of A Novel and Improved Thermosensitive Liposome Formulated with DPPC and a Brij Surfactant Using a Robust in Vitro System. *J. Controlled Release* **2011**, *154*, 290−297.

(21) Lindner, L. H.; Hossann, M.; Vogeser, M.; Teichert, N.; Wachholz, K.; Eibl, H.; Hiddemann, W.; Issels, R. D. Dual Role Of Hexadecylphosphocholine Miltefosine in Thermosensitive Liposomes: Active Ingredient and Mediator of Drug Release. *J. Controlled Release* **2008**, *125*, 112−120.

(22) Ta, T.; Convertine, A.J.; Reyes, C. R.; Stayton, P. S.; Porter, T. M. Thermosensitive Liposomes Modified with Poly(N-isopropylacrylamide-co-propylacrylic acid) Copolymers for Triggered Release of Doxorubicin. *Biomacromolecules* **2010**, *11*, 1915−1920.

(23) *ThermoDox*, Celsion Corp., Lawrenceville, NJ, USA, http://celsion.com/docs/technology_thermodox (accessed May 5, 2016).

DOI: 10.1021/acs.jpcb.6b02783
J. Phys. Chem. B XXXX, XXX, XXX−XXX

(24) Bratton, D. L.; Harris, R. A.; Clay, K. L.; Henson, P. M. Effects of Platelet Activating Factor and Related Lipids on Phase Transition of Dipalmitoylphosphatidylcholine. *Biochim. Biophys. Acta, Biomembr.* **1988**, *941*, 76−82.
(25) Torrecillas, A.; Aroca-Aguilar, J. D.; Aranda, F. J.; Gajate, C.; Mollinedo, F.; Corbalán-García, S.; de Godos, A.; Gómez-Fernández, J. C. Effects of the Anti-Neoplastic Agent ET-18-OCH3 and Some Analogs on the Biophysical Properties of Model Membranes. *Int. J. Pharm.* **2006**, *318*, 28−40.
(26) Huang, C.-H.; Mason, J. T. Structure and Properties of Mixed-Chain Phospholipid Assemblies. *Biochim. Biophys. Acta, Rev. Biomembr.* **1986**, *864*, 423−470.
(27) Bunker, A.; Magarkar, A.; Viitala, T. Rational Design of Liposomal Drug Delivery Systems, A Review: Combined Experimental and Computational Studies of Lipid Membranes, Liposomes and Their PEGylation. *Biochim. Biophys. Acta, Biomembr.* **2016**, DOI: 10.1016/j.bbamem.2016.02.025.
(28) Olson, F.; Hunt, C. A.; Szoka, F. C.; Vail, W. J.; Papahadjopoulos, D. Preparation of Liposomes of Defined Size Distribution by Extrusion through Polycarbonate Membranes. *Biochim. Biophys. Acta, Biomembr.* **1979**, *557*, 9−23.
(29) MacDonald, R. C.; MacDonald, R. I.; Menco, B. Ph. M.; Takeshita, K.; Subbarao, N. K.; Hu, L.-R. Small-Volume Extrusion Apparatus for Preparation of Large, Unilamellar Vesicles. *Biochim. Biophys. Acta, Biomembr.* **1991**, *1061*, 297−303.
(30) Allen, T. M.; Cleland, L. G. Serum-Induced Leakage of Liposome Contents. *Biochim. Biophys. Acta, Biomembr.* **1980**, *597*, 418−426.
(31) Hossann, M.; Wang, T.; Wiggenhorn, M.; Schmidt, R.; Zengerle, A.; Winter, G.; Eibl, H.; Peller, M.; Reiser, M.; Issels, R. D.; et al. Size of Thermosensitive Liposomes Influences Content Release. *J. Controlled Release* **2010**, *147*, 436−443.
(32) Shimanouchi, T.; Ishii, H.; Yoshimoto, N.; Umakoshi, H.; Kuboi, R. Calcein Permeation across Phosphatidylcholine Bilayer Membrane: Effects of Membrane Fluidity, Liposome Size, and Immobilization. *Colloids Surf., B* **2009**, *73*, 156−160.
(33) Tagami, T.; Ernsting, M. J.; Li, S.-D. Efficient Tumor Regression by a Single and Low Dose Treatment with a Novel and Enhanced Formulation of Thermosensitive Liposomal Doxorubicin. *J. Controlled Release* **2011**, *152*, 303−309.
(34) Jo, S.; Lim, J. B.; Klauda, J. B.; Im, W. CHARMM-GUI Membrane Builder for Mixed Bilayers and Its Application to Yeast Membranes. *Biophys. J.* **2009**, *97*, 50−58.
(35) Salomon-Ferrer, R.; Case, D. A.; Walker, R. C. An Overview of the Amber Biomolecular Simulation Package. *Wiley Interdiscip. Rev. Comput. Mol. Sci.* **2013**, *3*, 198−210.
(36) Dickson, C. J.; Madej, B. D.; Skjevik, Å. A.; Betz, R. M.; Teigen, K.; Gould, I. R.; Walker, R. C. Lipid14: The Amber Lipid Force Field. *J. Chem. Theory Comput.* **2014**, *10*, 865−879.
(37) Jorgensen, W. L.; Chandrasekhar, J.; Madura, J. D.; Impey, R. W.; Klein, M. L. Comparison of Simple Potential Functions for Simulating Liquid Water. *J. Chem. Phys.* **1983**, *79*, 926−935.
(38) Skjevik, Å. A.; Madej, B. D.; Walker, R. C.; Teigen, K. LIPID11: A Modular Framework for Lipid Simulations Using Amber. *J. Phys. Chem. B* **2012**, *116*, 11124−11136.
(39) Salomon-Ferrer, R.; Götz, A. W.; Poole, D.; Le Grand, S.; Walker, R. C. Routine Microsecond Molecular Dynamics Simulations with AMBER on GPUs. 2. Explicit Solvent Particle Mesh Ewald. *J. Chem. Theory Comput.* **2013**, *9*, 3878−3888.
(40) Le Grand, S.; Götz, A. W.; Walker, R. C. SPFP: Speed without Compromise—A Mixed Precision Model for GPU Accelerated Molecular Dynamics Simulations. *Comput. Phys. Commun.* **2013**, *184*, 374−380.
(41) Roe, D. R.; Cheatham, T. E. PTRAJ and CPPTRAJ: Software for Processing and Analysis of Molecular Dynamics Trajectory Data. *J. Chem. Theory Comput.* **2013**, *9*, 3084−3095.
(42) Taylor, K. M. G.; Morris, R. M. Thermal Analysis of Phase Transition Behaviour in Liposomes. *Thermochim. Acta* **1995**, *248*, 289−301.
(43) Biltonen, R. L.; Lichtenberg, D. The Use of Differential Scanning Calorimetry As a tool To Characterize Liposome Preparations. *Chem. Phys. Lipids* **1993**, *64*, 129−142.
(44) Suurkuusk, J.; Lentz, B. R.; Barenholz, Y.; Biltonen, R. L.; Thompson, T. E. A Calorimetric and Fluorescent Probe Study of the Gel−Liquid Crystalline Phase Transition in Small, Single-Lamellar Dipalmitoylphosphatidylcholine Vesicles. *Biochemistry* **1976**, *15*, 1393−1401.
(45) Spink, C. H. Differential Scanning Calorimetry. *Methods Cell Biol.* **2008**, *84*, 115−141.
(46) Koynova, R.; Caffrey, M. Phases and Phase Transitions of the Phosphatidylcholines. *Biochim. Biophys. Acta, Rev. Biomembr.* **1998**, *1376*, 91−145.
(47) Mouritsen, O. G.; Jørgensen, K. Dynamical Order and Disorder in Lipid Bilayers. *Chem. Phys. Lipids* **1994**, *73*, 3−25.
(48) Ortiz, A.; Gómez-Fernández, J. C. A Differential Scanning Calorimetry Study of the Interaction of Free Fatty Acids with Phospholipid Membranes. *Chem. Phys. Lipids* **1987**, *45*, 75−91.
(49) Ceckler, T. L.; Cunningham, B. A. Transition State Thermodynamics of Lipid Bilayers Characterized by Differential Scanning Calorimetry. *Chem. Educ.* **1997**, *2*, 1−17.
(50) Ambrosini, A.; Bossi, G.; Dante, S.; Dubini, B.; Gobbi, L.; Leone, L.; Bossi, M. G. P.; Zolese, G. Lipid-Drug Interaction: Thermodynamic and Structural Effects of Antimicotic Fluconazole on DPPC Liposomes. *Chem. Phys. Lipids* **1998**, *95*, 37−47.
(51) Heimburg, T. *Thermal Biophysics of Membranes*; Wiley-VCH Verlag GmbH: Weinheim, Germany, 2007.
(52) Ponce, A. M.; Vujaskovic, Z.; Yuan, F.; Needham, D.; Dewhirst, M. W. Hyperthermia Mediated Liposomal Drug Delivery. *Int. J. Hyperthermia* **2006**, *22*, 205−213.
(53) Ueno, M.; Yoshida, S.; Horikoshi, I. Characteristics of Membrane Permeability of Temperature-Sensitive Liposome. *Bull. Chem. Soc. Jpn.* **1991**, *64*, 1588−1593.
(54) Tieleman, D. P.; Marrink, S. J.; Berendsen, H. J. A Computer Perspective of Membranes: Molecular Dynamics Studies of Lipid Bilayer Systems. *Biochim. Biophys. Acta, Rev. Biomembr.* **1997**, *1331*, 235−270.
(55) Scott, H. L. Modeling the Lipid Components of Membranes. *Curr. Opin. Struct. Biol.* **2002**, *12*, 495−502.
(56) Hofsäß, C.; Lindahl, E.; Edholm, O. Molecular Dynamics Simulations of Phospholipid Bilayers with Cholesterol. *Biophys. J.* **2003**, *84*, 2192−2206.
(57) Kučerka, N.; Nieh, M.-P.; Katsaras, J. Fluid Phase Lipid Areas and Bilayer Thicknesses of Commonly Used Phosphatidylcholines As a Function of Temperature. *Biochim. Biophys. Acta, Biomembr.* **2011**, *1808*, 2761−2771.
(58) Kučerka, N.; Tristram-Nagle, S.; Nagle, J. F. Closer Look at Structure of Fully Hydrated Fluid Phase DPPC Bilayers. *Biophys. J.* **2006**, *90*, L83−L85.
(59) Nagle, J. F.; Tristram-Nagle, S. Structure of Lipid Bilayers. *Biochim. Biophys. Acta, Rev. Biomembr.* **2000**, *1469*, 159−195.
(60) Kučerka, N.; Nagle, J. F.; Sachs, J. N.; Feller, S. E.; Pencer, J.; Jackson, A.; Katsaras, J. Lipid Bilayer Structure Determined by the Simultaneous Analysis of Neutron and X-ray Scattering Data. *Biophys. J.* **2008**, *95*, 2356−2367.
(61) Vaz, W. L. C.; Clegg, R. M.; Hallmann, D. Translational Diffusion of Lipids in Liquid Crystalline Phase Phosphatidylcholine Multibilayers. A Comparison of Experiment with Theory. *Biochemistry* **1985**, *24*, 781−786.
(62) Scheidt, H. A.; Huster, D.; Gawrisch, K. Diffusion of Cholesterol and Its Precursors in Lipid Membranes Studied by 1H Pulsed Field Gradient Magic Angle Spinning NMR. *Biophys. J.* **2005**, *89*, 2504−2512.
(63) Poger, D.; Mark, A. E. Lipid Bilayers: The Effect of Force Field on Ordering and Dynamics. *J. Chem. Theory Comput.* **2012**, *8*, 4807−4817.
(64) Heimburg, T. Lipid Ion Channels. *Biophys. Chem.* **2010**, *150*, 2−22.

DOI: 10.1021/acs.jpcb.6b02783
J. Phys. Chem. B XXXX, XXX, XXX−XXX

(65) Blok, M. C.; Van Der Neut-Kok, E. C. M.; Van Deenen, L. L. M.; De Gier, J. The Effect of Chain Length and Lipid Phase Transitions on the Selective Permeability Properties of Liposomes. *Biochim. Biophys. Acta, Biomembr.* **1975**, *406*, 187−196.
(66) Zhelev, D. V. Material Property Characteristics for Lipid Bilayers Containing Lysolipid. *Biophys. J.* **1998**, *75*, 321−330.
(67) Ickenstein, L. M.; Arfvidsson, M. C.; Needham, D.; Mayer, L. D.; Edwards, K. Disc Formation in Cholesterol-Free Liposomes During Phase Transition. *Biochim. Biophys. Acta, Biomembr.* **2003**, *1614*, 135−138.
(68) Linden, C. D.; Wright, K. L.; McConnell, H. M.; Fox, C. F. Lateral Phase Separations in Membrane Lipids and the Mechanism of Sugar Transport in Escherichia coli. *Proc. Natl. Acad. Sci. U. S. A.* **1973**, *70*, 2271−2275.
(69) Nagle, J. F.; Scott, H. L., Jr. Lateral Compressibility of Lipid Mono- and Bilayers. Theory of Membrane Permeability. *Biochim. Biophys. Acta, Biomembr.* **1978**, *513*, 236−243.
(70) Fuchs, B.; Schiller, J.; Wagner, U.; Häntzschel, H.; Arnold, K. The Phosphatidylcholine/Lysophosphatidylcholine Ratio in Human Plasma Is an Indicator of the Severity of Rheumatoid Arthritis: Investigations by ^{31}P NMR and MALDI-TOF MS. *Clin. Biochem.* **2005**, *38*, 925−933.
(71) Marathe, G. K.; Ribeiro Silva, A.; de Castro Faria Neto, H. C.; Tjoelker, L. W.; Prescott, S. M.; Zimmerman, G. A.; McIntyre, T. M. Lysophosphatidylcholine and Lyso-PAF Display PAF-like Activity Derived from Contaminating Phospholipids. *J. Lipid Res.* **2001**, *42*, 1430−1437.
(72) Tjoelker, L. W.; Wilder, C.; Eberhardt, C.; Stafforinit, D. M.; Dietsch, G.; Schimpf, B.; Hooper, S.; Trong, H. L.; Cousens, L. S.; Zimmerman, G. A.; et al. Anti-inflammatory Properties of a Platelet-Activating Factor Acetylhydrolase. *Nature* **1994**, *374*, 549−553.
(73) Torrecillas, A.; Aroca-Aguilar, J. D.; Aranda, F. J.; Gajate, C.; Mollinedo, F.; Corbalán-García, S.; de Godos, A.; Gómez-Fernández, J. C. Effects of the Anti-neoplastic Agent ET-18-OCH3 and Some Analogs on the Biophysical Properties of Model Membranes. *Int. J. Pharm.* **2006**, *318*, 28−40.

DOI: 10.1021/acs.jpcb.6b02783
J. Phys. Chem. B XXXX, XXX, XXX−XXX